CORROSION SCIENCE AND TECHNOLOGY, Vol.21, No.2(2022), pp.77~88
[Research Paper]
pISSN 1598-6462 / eISSN 2288-6524
DOI: https://doi.org/10.14773/cst.2022.21.2.77

Corrosion Protection Effectiveness and Adsorption Performance of Schiff Base-Quinazoline on Mild Steel in HCl Environment

Firas F. Sayyid[1], Ali M. Mustafa[1], Mahdi M. Hanoon[1], Lina M. Shaker[2], and Ahmed A. Alamiery[2,3,†]

[1]*Department of production Engineering and metallurgical, University of technology-Iraq, Baghdad 10001, Iraq*
[2]*Department of Chemical and Process Engineering, Faculty of Engineering and Build Environment, Universiti Kebangsaan Malaysia, 43000 UKM Bangi, Selangor, Malaysia*
[3]*Energy and Renewable Technology Centre, University of Technology, Baghdad, Iraq*
(Received November 04, 2021; Revised April 02, 2022; Accepted April 06, 2022)

Schiff base quinazoline derivative viz., 3-((2-hydroxy-3-methoxybenzylidene)amino)-2-methylquinazolin-4(3H)-one (SB-Q), was synthesized in this study. Its corrosion protection impact on mild steel (MS) in 1 M hydrochloric acid solution was examined by performing weight loss measurements. The protective efficacy of SB-Q on MS in 1 M HCl was investigated based on its concentrations, immersion period, and immersion temperature. SB-Q was found to be an efficient inhibitor for the corrosion of MS. Its inhibition efficiency was improved by increasing the concentration of SB-Q to an optimal concentration of 500 ppm. Its inhibition efficacy was 96.3% at 303 K. Experimental findings revealed that its inhibition efficiency was increased with increasing immersion time, but decreased with an increase in temperature. The adsorption of SB-Q molecules was followed the Langmuir adsorption isotherm model. The adsorption of the examined inhibitor molecules on the surface of mild steel was studied by density functional theory (DFT). DFT investigation confirmed weight loss findings.

Keywords: *Corrosion inhibitor, Mild steel, Methylquinazolin, Schiff Base, DFT*

1. Introduction

Mild steel is commonly applied to fabricate various materials in a type of industry. Although mild steel inexpensive and have proper mechanical characteristics in various manufacturing purposes, it is likely to the corrosion [1,2]. The numerous efficient strategies to control and/or retard the corrosion in a closed environment is the corrosion inhibitors addition to acidic environments. Difference natural or synthetic organic inhibitors present a chance for efficient alloys in various applications for acidic solutions. With the different industrial acidic solutions, HCl is usually used for various manufacturing purposes. HCl is widely utilized for pickling, descaling, cleaning, and mild steel etching [3,4]. Despite this, the HCl medium is understood to be extremely corrosive for different alloys. Mild steel is recognized as a great achievement manufacturing alloy in a considerable industry. In severe industrial applications, the immediate interaction of HCl solution with mild steel leads to corrosion [5,6]. Quantum chemical approaches were previously identified as a very useful technique in managing the molecular structure and explaining the electronic structure as well as the interaction that may be useful in mapping novel inhibitory molecules with great efficiency through the molecular structure relationship and activity approach. Quantitative chemical computation through density functional theory is an appropriate technique and these often feasible general means have enabled corrosion investigators to computationally study the corrosion inhibition mechanism [7,8]. Calculations have been extensively applied to investigate the molecular electronic structures of a broad spectrum of inhibitors adsorption models utilizing several quantum parameters, which has provided valuable physical visions on adsorption mechanisms corrosion inhibition [9,10]. Therefore, protection performance is related to the molecular parameters which can be achieved by a computational approach such as chemical reactivity, and atomic charges [11,12]. Other theoretical findings are the energy of higher occupied molecular orbital (EHOMO), the energy of lower

[†]Corresponding author: dr.ahmed1975@gmail.com, dr.ahmed1975@ukm.edu.my

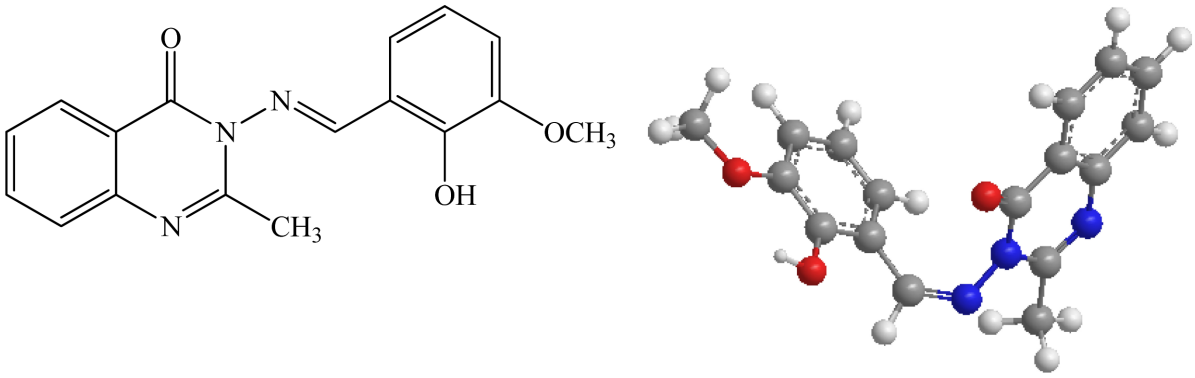

Molecular structure Geometrical optimized structure

Fig. 1. (a) molecular structure of the SB-Q, (b) geometrical optimized structure of SB-Q molecule

Table 1. Chemical composition of the mild steel coupon (wt%)

Carbon	Manganese	Silicon	Aluminum	Sulfur	Phosphorus	Iron
0.210	0.050	0.380	0.010	0.050	0.090	balance

unoccupied molecular orbital (LUMO), electronegativity, chemical softness, chemical hardness, and electron transfer number [13,14]. This investigation centered on the study of the corrosion inhibitive efficacy of a new corrosion inhibitor namely 3-((2-hydroxy-3-methoxybenzylidene)amino)-2-methylquinazolin-4(3H)-one (SB-Q) on mild steel in HCl media. Therefore, the suggested corrosion inhibition mechanism and the adsorption nature of SB-Q molecules on the surface of mild steel are explained in detail based on the realized outcomes from weight loss measurements, adsorption isotherm study, and DFT studies. Fig. 1 exhibits the molecular structure of the studied inhibitor and it optimized structure.

2. Material and methods

2.1 Materials

The inhibitory effects of SB-Q are examined on mild steel with the chemical composition presented in Table 1.

The mild steel test coupons rectangular shapes, which have the dimensions of 4.5 cm × 2 cm × 1.5 cm were sliced and smoothed for weight loss methods with sandpaper of different grades. Before investigations, mild steel coupons had been washed with the bi-distilled water, thoroughly cleaned in acetone, and drained using a desiccator.

2.2 Tested solutions

The weight loss tests were achieved out in a freshly prepared 1 M HCl environment (a non-stirred, aerated, and 37% analytical grade) utilizing bi-distilled water. The concentrations of freshly prepared inhibitor ranged from 100 ppm to 600 ppm as 1, 5, 10, 24, and 48 hours of immersion, with temperatures varying from 303 to 333 K and solution volumes of 250 mL. Each test was performed three times and the mean repeatability of the measurements was given.

2.3 Weight loss techniques

In order to determine the corrosion rate analyses, mass loss techniques were conducted. It was completed following the recommended technique ASTM [15]. The weight loss techniques have been conducted below distinct temperature situations. The specimens were immersed in a glass cell, in an aerated environment having the HCl without and with the addition of various concentrations of the tested inhibitor to let the solution to be preserved at the required temperature. Before every experiment, the mild steel coupons are regularly polished, completely washed with bi-distilled water, washed with acetone and dried in the desiccator. The tested coupons were weighed accurately applying an accuracy balance. Following initial balancing, the coupons were exposed to

corrosive media in the absence and presence of the various concentrations of tested inhibitor. After (1, 5, 10, 24, and 48 h) of exposure periods, the mild steel coupons were rinsed repeatedly with distilled water, washed with acetone, dried, and weighed. The weight loss analyses have been conducted at temperatures of 303, 313, 323, and 333 K. All the tests were repeated three times, and the average was taken. The weight loss analyses global principles were based on the determination of the mass loss per specimen regarding the immersion time in HCl media that is maintained at a determined temperature. The rate of corrosion was calculated according to equation (1) [16];

$$C_R = \frac{K \times W}{a \times t \times p} \quad (1)$$

As described by the approved techniques: ASTM, $\rho = 7.89\ cm^{-3}$, $K = 8.76 \times 10^4$, W refers to the weight loss in gm, t signifies to the exposure period in h., and a is the mild steel coupon area in cm^2.

The exposure mild steel coupon area was determined according to equation (2):

$$a = \frac{\pi}{2}(D^2 - d^2) + \frac{\pi}{D} + l\pi d \quad (2)$$

where D is the coupon diameter, d represents the holding hole diameter, and l refers to coupon thickness

The inhibitor efficiency (IE%) and the surface coverage (θ) were calculated according to equations (3) and (4) [17],

$$IE\% = \left(1 - \frac{C_R}{C_R^o}\right) \times 100 \quad (3)$$

$$\theta = \left(1 - \frac{C_R}{C_R^o}\right) \quad (4)$$

where C_R^o the corrosion rate in absence of tested inhibitor whereas C_R represents the corrosion rate in presence of tested inhibitor

2.4 DFT

The theoretical quantum simulation approach was achieved by utilizing density functional theory (DFT) to investigate the inhibitor molecules' electronic structures to determine the theoretical characteristics of inhibitor molecules. The optimized geometrical structure of inhibitor molecules was achieved by applying DFT/B3LYP with basis set 6-31G [18-21]. Physical parameters such as the energy of highest occupied molecular orbital energy (E_{HOMO}), energy of lowest unoccupied molecular orbital energy (E_{LUMO}), energy gap $\Delta E = E_{HOMO} - E_{HOMO}$, ionization potential ($I$), electronic affinity ($A$), electronegativity ($\chi$), chemical hardness ($\eta$), chemical softness ($\sigma$), and the electron transfer fraction (ΔN) were calculated according to equations (5) to (10) [22];

$$I = -E_{HOMO} \quad (5)$$

$$A = -E_{LUMO} \quad (6)$$

$$\chi = \frac{\Delta E}{2} \quad (7)$$

$$\eta = \frac{E_{HOMO} - E_{LUMO}}{2} \quad (8)$$

$$\sigma = \frac{1}{\eta} \quad (9)$$

$$\Delta N = \frac{\phi_{Fe} - \chi_{inh}}{2(\eta_{Fe} - \eta_{inh})} \quad (10)$$

where $\phi_{Fe} = 4.82\ eV$, $\eta_{Fe} = 0$.

3. Results and Discussion

3.1 Gravimetric analyses

3.1.1 Concentration effect

The subject of the inhibition performance of the SB-Q molecules toward the mild steel corrosion in a 1 M hydrochloric acid environment 1.0 M HCl, with weight loss measurements, was carried at 303 K and for the various concentrations for 1, 5, 10, 24, 48 and 72 h exposure times. Fig. 2 exhibits the evaluated weight loss findings for the different concentrations and various exposure times of SB-Q [23]. The determination of the weight loss findings obviously shows that the SB-Q molecule has superior corrosion inhibition characteristics for mild steel in 1 M HCl solution. Moreover, the inhibition efficiency increases with the SB-Q concentration increase. Certainly, at 500 ppm, SB-Q has the highest inhibition efficacy of 96.3%. It was remarked that the rate of corrosion reduces while the inhibition efficiency is improved with an addition of SB-Q. Experimental

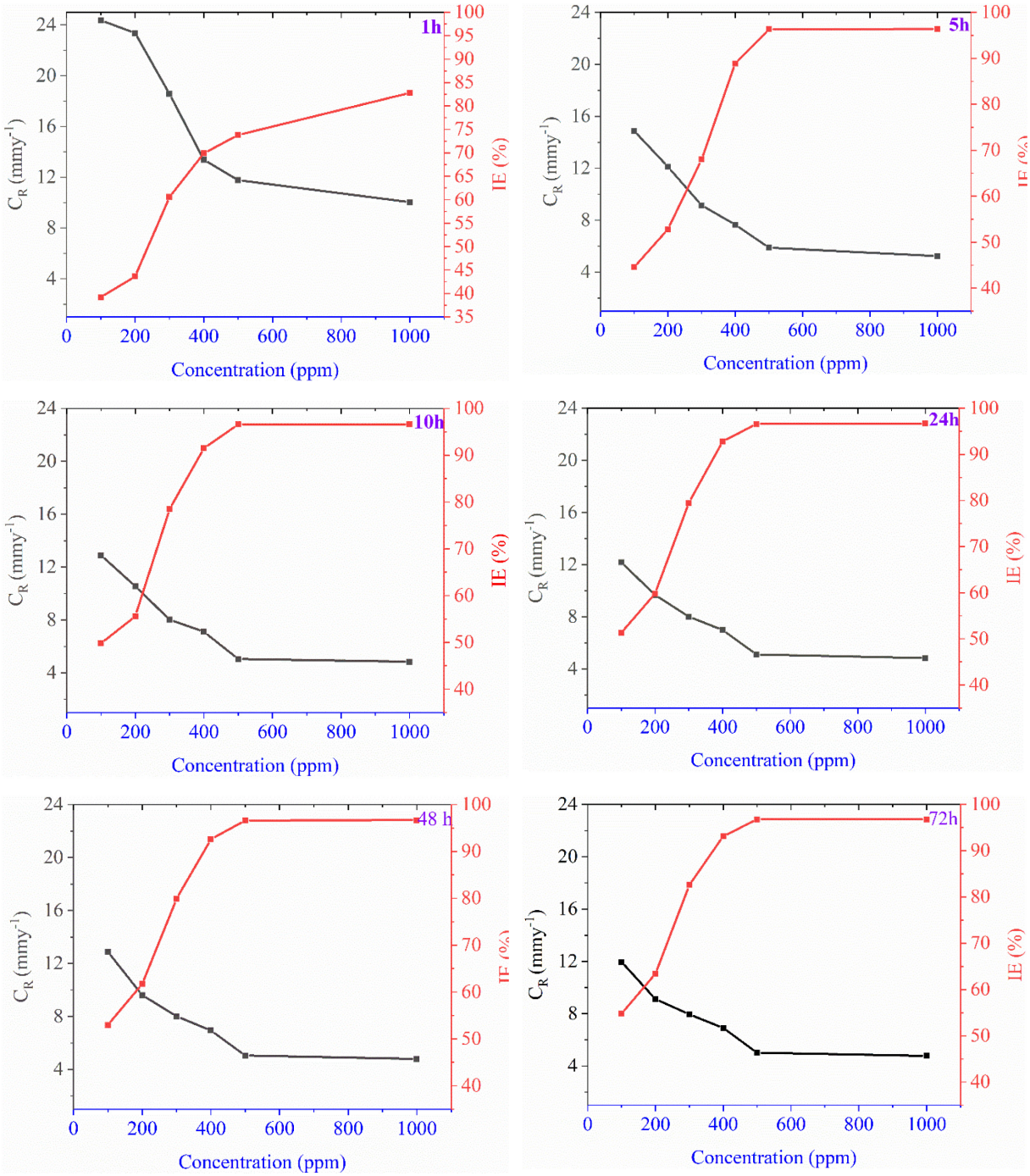

Fig. 2. The rate of corrosion rate and inhibition efficiency of the tested inhibitor at different concentrations (100-1000 ppm) for mild steel versus the immersion time (1-72 h), at 303 K

findings data show that SB-Q is adsorbed on the mild steel surface efficiently, which is the basis for successful protection from corrosion. Fig. 2 exhibits that variations in inhibition efficiency for different inhibitor concentrations were depend on the immersion period. With the addition of SB-Q, the protection efficacy of SB-Q was firstly increased in the corrosive solution with the exposure period reaching a maximum level where the efficacy probably means constant regardless of inhibitor concentration [24,25]. This behavior can be explained by the fact that there are a limited number of sites available. As a result, it was discovered that the addition of the

Table 2. SB-Q inhibitory efficiency was compared quantitatively to that of other Schiff bases recently examined

No.	Inhibitor	IE%	Ref.
1	SB-Q	96	-
2	3-pyridinecarboxaldehyde-4-phenyl thiosemicarbazide	96	30
3	4-pyridinecarboxaldehyde-4-phenylthiosemicarbazide	93	30
4	3-mercapto-2-((4-methoxybenzylidene)amino)propanoic acid	66	31
5	2-((4-hydroxy-3-methoxybenzylidene)amino)-3-mercaptopropanoic acid	77	31
6	3-mercapto-2-(((E)-3-phenylallylidene)amino)propanoic acid	97	31
7	3-((4-(dimethylamino)benzylidene)amino)-2-methylquinazolin-4(3H)-one	92	32
8	3-((4-hydroxybenzylidene)amino)-2-methylquinazolin-4(3H)-one	96	32
9	3-(phenylimino)indolin-2-one	72	33
10	3,3- (1,4-phenylenebis (azan-1-yl-1-ylidene))diindolin-2-one	84	33
11	L400	92	34
12	L600	94	34
13	N,N′-(1,4-phenylenebis(methanylylidene))bis(5-(methylthio)-1,3,4-thiadiazol-2-amine)	92	35
14	5,5′-((1,4-phenylenebis(methanylylidene))bis(azanylylidene))bis(1,3,4-thiadiazole-2-thiol)	91	35
15	N,N′-(1,4-phenylenebis(methanylylidene))bis(5-methyl-1,3,4-thiadizol-2-amine)	87	35
16	N,N′-(1,4-phenylenebis(methanylylidene))bis(1,3,4-thiadiazol-2-amine)	80	35
17	N'-[4-(dimethylamino) benzylidene]-4-hydroxybenzohydrazide	83	36

investigated inhibitor reduces the mass loss of the metal and delays its development with the immersion time, affecting its efficiency as shown in Fig. 2.

In HCl solutions, the inhibition efficacy of the current inhibitor (SB-Q) can be compared with other reported inhibitors that use corrosion inhibitors derived from Schiff bases to protect the corrosion of mild steel. Table 2 shows that the majority of Schiff bases examined have strong inhibitory efficacy. In order to make the comparison with the current inhibitor in question, SB-Q has the greatest inhibitory efficiency compared to all Schiff bases mentioned in Table 2 [26-28], as well as an efficiency equivalent to that described in [29]. It is obvious that when the concentration of SB-Q increased, the rate of corrosion reduced and the inhibitive efficacy improved. This could be because the inhibitor's adsorption coverage on mild steel surfaces increases as the SB-Q concentration increased.

3.1.2 Temperature Effect

To determine, the impact of temperature on the inhibition efficiency, the tests were performed at four various temperatures levels of (303, 313, 323, and 333 K)

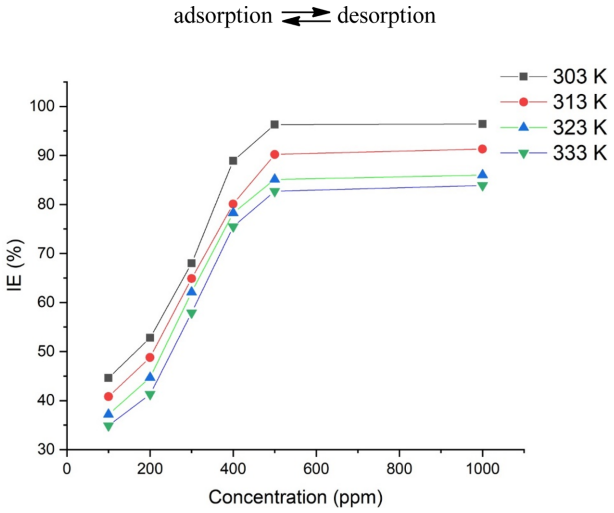

Fig. 3. The inhibition efficiency of the tested inhibitor at different concentrations (100-1000 ppm) for mild steel versus the Temperature (303-333 k), for 5 h as immersion time

in 1 M hydrochloric acid solution containing six concentrations (100, 200, 300, 400, 500 and 1000 ppm) of tested inhibitor for 5 h as immersion time. Fig. 3, exhibits the corrosion inhibition results as a temperature function for 5 h as immersion time. From the experimental

findings, it is obvious that values of protection efficacy in the existence of the various concentrations of tested inhibitor in 1.0 M HCl decrease with increasing temperature from 303 to 333 K. The inhibitory efficiency is temperature-dependent and diminishes with increasing temperature, showing that at higher temperatures, mild steel dissolution predominates on the mild steel surface [37]. This phenomenon is attributed to the fact that the adsorption mechanism weakens at high temperatures, implying physical adsorption. The rise in temperature may stimulate higher metal surface kinetic energy, which has a detrimental influence on the adsorption process, weakening it and encouraging desorption, resulting in the equilibrium shift toward desorption as shown below,

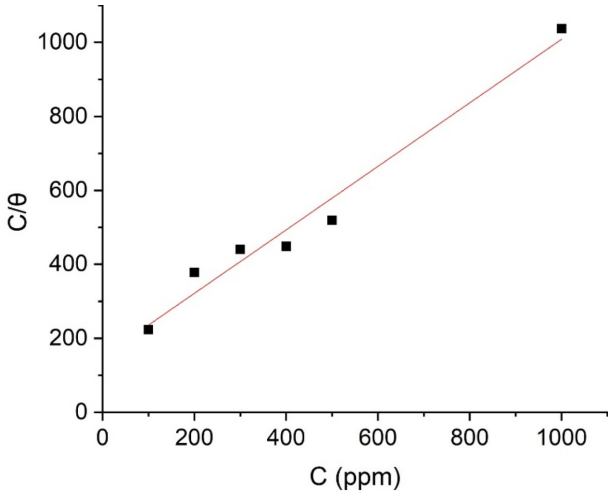

Fig. 4. Langmuir adsorption isotherm plot for various concentration at 303 K

3.2 Adsorption isotherm

Adsorption isotherms are explored in order to define the possible mechanism of interaction between molecules inhibiting corrosion with the mild steel surface. The collected information was adapted in order to identify the best fits to the most common adsorption isotherms: Temkins, Freundlich, and Langmuir. Temkins, Freundlich and Langmui isotherm models fit the experimental findings, although Langmuir's adsorption isotherm is most suitable. The inhibitor adsorption on a mild steel surface is followed by Langmuir Isotherm in a corrosive environment.

Langmuir isotherm model can be presented by equation (11) [38]:

$$\frac{C}{\theta} = \frac{1}{K_{ads}} + C \tag{11}$$

where C represents tested inhibitor concentration, θ signifies to surface coverage and K_{ads} refers to the equilibrium constant.

The plot of concentration (C) against C/θ at 303 K is described in Fig. 4. The experiment's findings of the adsorption of the tested inhibitor molecules shown by linear plot at 303 K confirms the opportunity for the approach of tested inhibitor molecules adsorption by Langmuir isotherm model. Usually, the inhibitive efficacy with a high value of a specific corrosion inhibitor is approved by a higher value of K_{ads} determined from the intercept which is relevant to its more favorable binding characteristics on the mild steel surface Langmuir isotherm model revealed that heteroatoms (nitrogen and oxygen) in tested inhibitor molecules interact by sharing their unpaired electrons with 3d-orbitals of iron atoms on the surface of mild steel. K_{ads} is depending on the temperature and reduces with the increases of temperature which suggests desorption process of inhibitor molecules on the mild steel surface. It is obvious that the correlation coefficient ($R^2 = 0.9858$) of the plot is closed to one which implies that tested inhibitor molecules which adsorbed on the mild steel surface obeys the Langmuir isotherm model. Despite, the slope ($slope = 0.858$), is closed to unity, means that the stimulation of Langmuir isotherm model was not ideal. The variation from one could be the interaction result of the adsorbed tested inhibitor molecules on the mild steel surface and unsaturated nuclei [39].

The free adsorption energy (ΔG^o_{ads}) might be determined based on equation (12),

$$K_{ads} = \frac{1}{55} EXP\left(\frac{\Delta G^o_{ads}}{RT}\right) \tag{12}$$

The external characteristic of the adsorption processes may be due to the rising of temperature and the inhibitor molecules may desorbed from the mild steel surface. As a result, the inhibition efficiency may decrease. This is obvious in Fig. 3 that represents the relation between inhibition efficiency and temperature. Generally, if the free energy (ΔG^o_{ads}) value of the adsorption reaction is

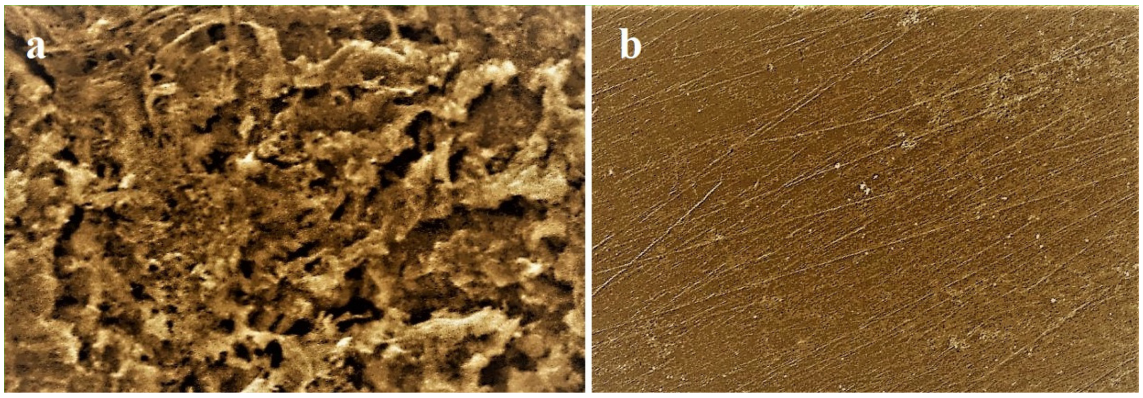

Fig. 5. SEM images of light steel coupon surfaces: (a) after 10 h exposure in 1.0 M HCl environment without addition of SB-Q, and (b) after 10 h exposure in 1.0 M HCl environment with addition of 500 ppm of SB-Q

up to -20 kJ.mol^{-1}, then the process of adsorption is carried by the physisorption, whereas if the free energy value of the adsorption reaction is below -40 kJ.mol^{-1} then the process of adsorption is conducted through chemisorption [40]. According to Equation 12, it is clear that the value of ΔG^{o}_{ads} is -34.8 kJ.mol^{-1} which confirms both mechanisms of physical and chemical adsorptions which are conducted through electrostatic interaction and chemical bonds.

3.3 Surface analysis

SEM analysis was performed using a Hitachi TM1000 benchtop microscope. In the SEM images, the coupons were immersed in the corrosion solution in the absence and presence of SB-Q as a corrosion inhibitor at a concentration of 500 ppm and 10 h as the immersion time.

Fig. 5 shows SEM images of light steel surface slips in 1.0 M HCl-free SB-Q solution and in the presence of SB-Q (a and b). After immersion for 10 h in 1.0 M HCl, Fig. 5a shows a slip of a mild steel surface severely damaged by immersion in HCl solution. Fig. 5b shows a SEM image after adding 500 ppm SB-Q to a 1.0 M HCl solution.

The surface of the mild steel was smooth and free of pits. It can be concluded that the corrosion rate is lower in the presence of SB-Q particles. These findings also support the results of weight loss and quantum chemical calculations.

3.4 Theoretical calculations

Frontier molecular orbitals (HOMO and LUMO) are valuable in suggesting the adsorption cities of the SB-Q molecules which have the ability to interact with a mild steel surface. The high-occupied molecular orbital (HOMO) and low unoccupied molecular orbital (LUMO) illustration of the investigated SB-Q molecules is presented in Fig. 6.

According to the energies of HOMO and LUMO, the empty 3d orbital of an iron atom on the surface of mild steel can receive the electron pairs from tested inhibitor molecules generally from nitrogen and oxygen atoms as providing cities in the inhibitor molecules. Furthermore, these molecules can receive electrons from iron atoms on the mild steel surface through the back bonding donation mechanism (from anti-bonding orbitals) [41]. These processes increase the inhibitor molecules adsorption onto the mild steel surface.

According to Koopman's theorem [22] the energy of HOMO is usually correlated with the ability to donate electrons of the molecule; E_{HOMO} high value is possible to indicate the inhibitor molecule's tendency to provide electrons to suitable acceptor particles. The value of E_{LUMO}, indicates the molecule's ability to receive an electron. With increased *HOMO* and decreased *LUMO* energy, the binding capacity of the inhibitor to the mild steel surface rises. The lower the E_{LUMO} value, the more likely it would be that electrons would be accepted by the molecule. In addition, an essential characteristic that controls the reactivity of the inhibitor molecule to the mild steel surface adsorption is also the energy gap between the *HOMO* and *LUMO* molecular orbits. As energy gap ($\Delta E = E_{HOMO} - E_{LUMO}$) decreases, the molecular interaction will increase which indicates an improvement in the

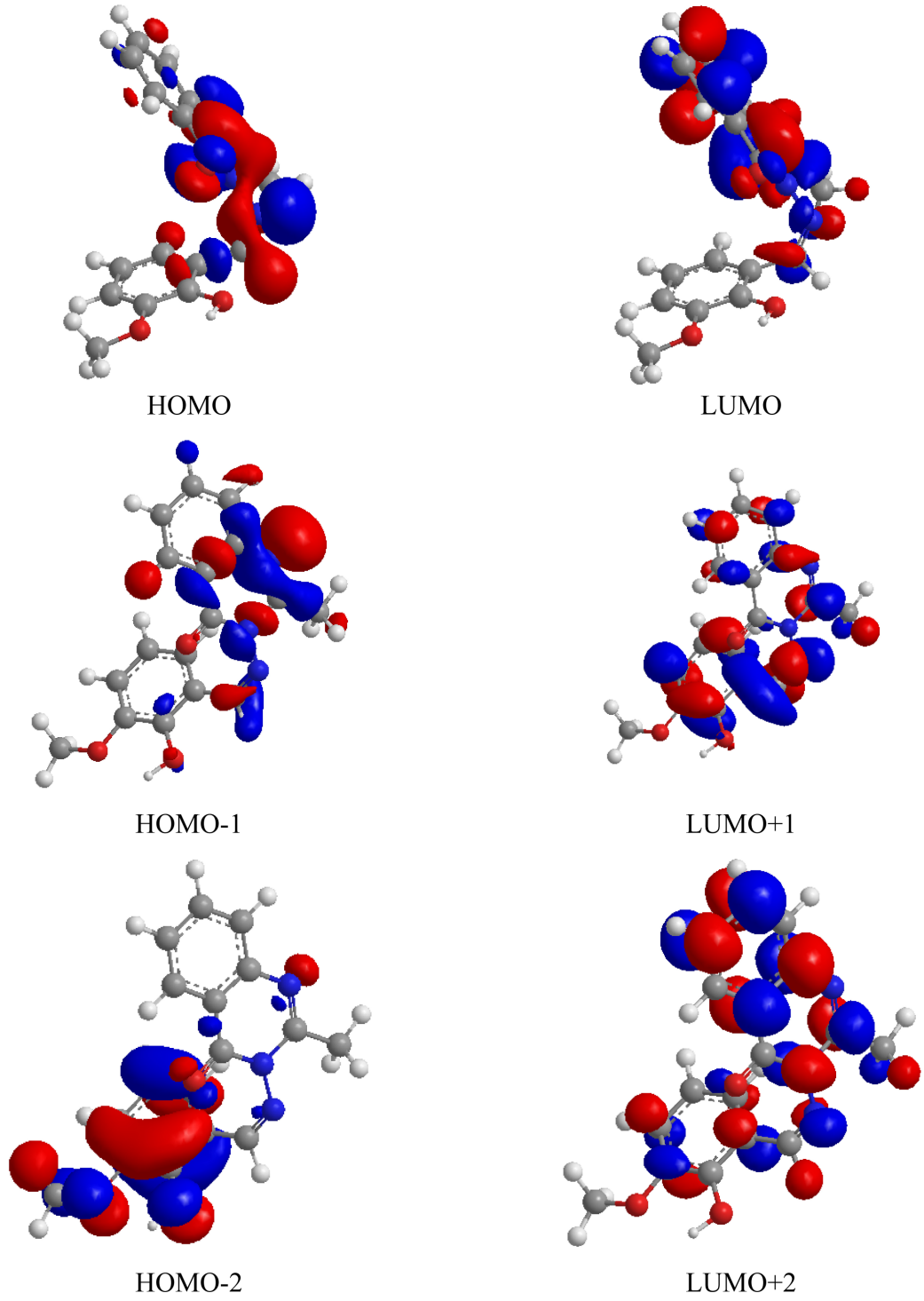

Fig. 6. Molecular Orbitals tested inhibitor molecules

protective performance of the tested inhibitor molecules. For efficient overlap, the variation between the orbitals energies usually should be low, and the whole variation between the E_{HOMO} - E_{LUMO} indicates the involvement in the mild steel−inhibitor interactions. Moreover, the variation between the E_{LUMO-2} and E_{LUMO-1} for the examined inhibitor molecules is very low approving the participation of E_{LUMO-1} and E_{LUMO-2} in the inhibitor molecules−mild steel surface interactions [42].

It is obvious from Table 3 that inhibitor molecules have

a high value of HOMO energy which indicates that the significant ability to donate an electron. It is obvious that the inhibitor molecules exhibit the lowest E_{LUMO}, the interaction of mild steel with inhibitor molecules. The estimates further confirm that inhibitor molecules form has the ΔE value (5.566 eV) suggesting that the tested inhibitor is the very active inhibitor which is readily adsorbed on the mild steel surface producing protecting layer. This matches with the weight loss findings that the tested inhibitor has a high inhibition efficiency on the surface of mild steel through coordination bonds and physical interactions. The Coordination bonds between the unpaired electrons and 3d-orbitals of iron atoms and the vacant 3d-orbital on mild steel surface. Absolute hardness, η, and softness, σ, are significant parameters to evaluate the stability and reactivity of molecules. A hard molecule has considerable band energy, and a soft molecule has low band energy [43].

The hard molecule is low reactive than a soft molecule because they readily donate electrons to the acceptor. For the transfer of electrons, adsorption may happen at the highest value of σ has the lowest value η. The result from Table 3 reveals that tested inhibitor molecules have a low band gap, high softness with low hardness; this conforms with the weight loss findings results that tested inhibitor molecules have a significant inhibition efficiency on the surface of mild steel. DFT is found to be significant in presenting indicates the electronegativity (χ), hardness (η), and softness (σ) which represented the chemical reactivity and selectivity of the molecule. Table 3 presents the computed quantum chemical parameters which present data about the reactive behavior of tested corrosion inhibitor [44].

3.4.1 Corrosion inhibition mechanism

Based on the experimental findings of corrosion protection of SB-Q in the 1 M HCl and also the theoretical investigation, a suggested adsorption mechanism was demonstrated in Fig. 7. Fig. 7 refers to the behavior of tested inhibitor molecules and adsorption process of SB-Q molecules toward the mild steel surface. Corrosion is a chemical process, and the behavior of the inhibitor molecules, achieved free electrons of inhibitor molecules transfer from the inhibitor molecules to the mild steel surface and forming a protective layer on the mild steel surface. On a similar process the examined inhibitor molecules have nitrogen and oxygen as heteroatoms and also have heterocyclic and phenyl rings in addition to p-electrons. The unpaired free electrons of SB-Q were

Table 3. Quantum chemical parameters of SB-Q molecule

Parameter	Value
I (Ionization potential)	8.613 eV
A (Electron affinity)	2.951 eV
ΔE (Band gap)	5.662 eV
E_{HOMO}	-8.613 eV
E_{HOMO-1}	-10.139 eV
E_{HOMO-2}	-11.217 eV
E_{LUMO}	-2.951 eV
E_{LUMO+1}	-2.243 eV
E_{LUMO+2}	-0.189 eV
χ (Elctronegativity)	2.831 eV
η (Global hardness)	5.782 eV
σ (Global softness)	0.1729
ΔE (Fractions of electron transferred)	0.1718

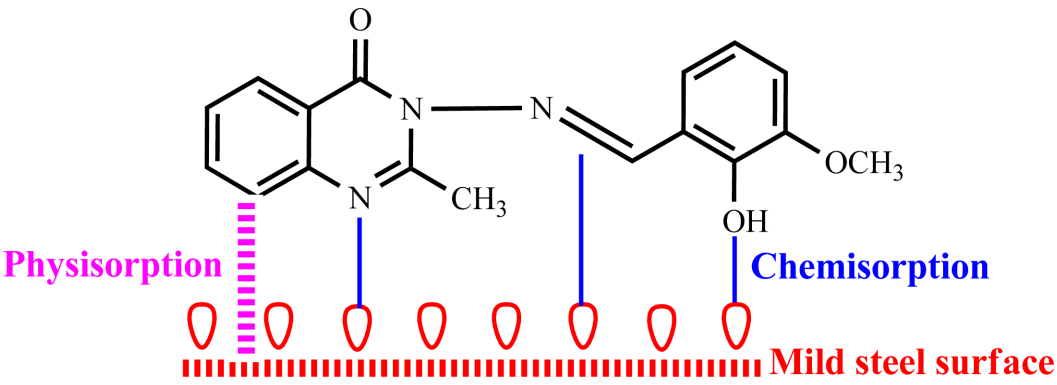

Fig. 7. Postulated inhibition mechanism of SB-Q on mild steel surface in corrosive medium

transfer to the unoccupied 3d- orbital of iron atoms on the surface of mild steel and forming coordination bonds (chemisorption). Furthermore, the aromatic ring of the SB-Q molecules interacts with surface of mild steel through Van der Waals forces (physisorption).

4. Conclusion

The synthesized quinazoline derivative exhibited good protection performance for the corrosion of mild steel in 1 M HCl environments and the inhibitive efficacy was determined to be concentration, immersion time, and temperature-dependent. Langmuir isotherm model was best fit the adsorption process for the investigated inhibitor molecules. The free energy has a negative sign value, and the negative value of Gibbs free energy of adsorption suggests that the adsorption of inhibitor molecules involves both physical and chemical adsorption process.

References

1. S. B. Al-Baghdadi, F. T. Noori, W. K. Ahmed, A. A. Al-Amiery, Thiadiazole as a potential corrosion inhibitor for mild steel in 1 M HCl, *Journal of Advanced Electrochemistry*, **2**, 67 (2016).
2. Q. A. Jawad, D. S. Zinad, R. D. Salim, A. A. Al-Amiery, T. S. Gaaz, M. S. Takriff, and A. A. H. Kadhum, Synthesis, characterization, and corrosion inhibition potential of novel thiosemicarbazone on mild steel in sulfuric acid environment, *Coatings*, **9**, 729 (2019). Doi: https://doi.org/10.3390/coatings9110729
3. A. A. Al-Amiery, M. H. Ahmed, T. A. Abdullah, T. S. Gaaz, A. A. Kadhum, Electrochemical studies of novel corrosion inhibitor for mild steel in 1 M hydrochloric acid, *Results in Physics*, **9**, 978 (2018). Doi: https://doi.org/10.1016/j.rinp.2018.04.004
4. H. T. Hussein, A. Kadhim, A. A. Al-Amiery, A. A. H. Kadhum, and A. B. Mohamad, Enhancement of the wear resistance and microhardness of aluminum alloy by Nd: YaG laser treatment, *The Scientific World Journal*, 2014, Article ID 842062 (2014). Doi: https://doi.org/10.1155/2014/842062
5. A. Y. Issa, K. S. Rida, A. Q. Salam, and A. A. Al-Amiery, Acetamidocoumarin as a based eco-friendly corrosion inhibitor, *International Journal of ChemTech Research*, **9**, 39 (2016). https://www.sphinxsai.com/2016/ch_vol9_no11/1/(39-47)V9N11CT.pdf
6. Salim RD, Jawad QA, Ridah KS, Shaker LM, Al-Amiery AA, Kadhum AA, Takriff MS. Corrosion inhibition of thiadiazole derivative for mild steel in hydrochloric acid solution, *International Journal of Corrosion and Scale Inhibition*, **9**, 550 (2020). Doi: https://dx.doi.org/10.17675/2305-6894-2020-9-2-10
7. A. A. Al-Amiery, L. M. Shaker, A. A. Kadhum, M. S. Takriff, Corrosion Inhibition of Mild Steel in Strong Acid Environment by 4-((5, 5-dimethyl-3-oxocyclohex-1-en-1-yl) amino) benzenesulfonamide, *Tribology in industry*, **42**, 89 (2020). Doi: https://doi.org/10.24874/ti.2020.42.01.09
8. A. Y. Musa, A. B. Mohamad, A. A. Al-Amiery, and L. T. Tien, Galvanic corrosion of aluminum alloy (Al2024) and copper in 1.0 M hydrochloric acid solution, *Korean Journal of Chemical Engineering*, **29**, 818 (2012). Doi: https://doi.org/10.1007/s11814-011-0233-z
9. A. Kadhim, A. A. Al-Amiery, R. Alazawi, M. K. S. Al-Ghezi, and R. H. Abass, Corrosion inhibitors. A review, *International Journal of Corrosion and Scale Inhibition*, **10**, 54 (2021). Doi: http://dx.doi.org/10.17675/2305-6894-2021-10-1-3
10. A. A. Al-Amiery, L. M. Shaker, Corrosion inhibition of mild steel using novel pyridine derivative in 1 M hydrochloric acid, *Koroze a Ochrana Materiálu*, **64**, 59 (2020). Doi: https://doi.org/10.2478/kom-2020-0009
11. A. Alamiery, E. Mahmoudi, and T. Allami, Corrosion inhibition of low-carbon steel in hydrochloric acid environment using a Schiff base derived from pyrrole: Gravimetric and computational studies, *International Journal of Corrosion and Scale Inhibition*, **10**, 749 (2021). Doi: http://dx.doi.org/10.17675/2305-6894-2021-10-2-17
12. Alamiery AA. Anticorrosion effect of thiosemicarbazide derivative on mild steel in 1 M hydrochloric acid and 0.5 M sulfuric Acid: Gravimetrical and theoretical studies, *Materials Science for Energy Technologies*, **4**, 263 (2021). Doi: https://doi.org/10.1016/j.mset.2021.07.004
13. R. D. Salim, N. Betti, M. Hanoon, A. A. Al-Amiery, 2-(2, 4-Dimethoxybenzylidene)-N-Phenylhydrazinecarbothioamide as an Efficient Corrosion Inhibitor for Mild Steel in Acidic Environment, *Progress in Color, Colorants and Coatings*, **15**, 45 (2022). Doi: https://dx.doi.org/10.30509/pccc.2021.166775.1105
14. L. M. Shaker, A. Al-Adili, A. A. Al-Amiery, and M. S. Takriff, The inhibition of mild steel corrosion in 0.5 M H_2SO_4 solution by N-phenethylhydrazinecarbothioamide (N-PHC), *Journal of Physics: Conference Series*, **1795**,

012009 (2021). Doi: https://doi.org/10.1088/1742-6596/1795/1/012009

15. ASTM G1 - 03, Standard practice for preparing, cleaning, and evaluating corrosion test specimens (2011). Doi: https://www.astm.org/g0001-03r11.html
16. D. S. Zinad, M. Hanoon, R. D. Salim, S. I. Ibrahim, A. A. Al-Amiery, M. S. Takriff, A. A. Kadhum, A new synthesized coumarin-derived Schiff base as a corrosion inhibitor of mild steel surface in HCl medium: gravimetric and DFT studies, *International Journal of Corrosion and Scale Inhibition*, **9**, 228 (2020). Doi: http://dx.doi.org/10.17675/2305-6894-2020-9-1-14
17. A. Al-Amiery, L. M. Shaker, A. A. Kadhum, M. S. Takriff, Synthesis, characterization and gravimetric studies of novel triazole-based compound, *International Journal of Low-Carbon Technologies*, **15**, 164 (2020). Doi: https://doi.org/10.1093/ijlct/ctz067
18. S. S. Al-Taweel, K. W. S. Al-Janabi, H. M. Luaibi, A. A. Al-Amiery, and T. S. Gaaz, Evaluation and characterization of the symbiotic effect of benzylidene derivative with titanium dioxide nanoparticles on the inhibition of the chemical corrosion of mild steel, *International Journal of Corrosion and Scale Inhibition*, **8**, 1149 (2019). Doi: http://dx.doi.org/10.17675/2305-6894-2019-8-4-21
19. T. A. Salman, A. A. Al-Amiery, L. M. Shaker, A. A. Kadhum, M. S. Takriff, A study on the inhibition of mild steel corrosion in hydrochloric acid environment by 4-methyl-2-(pyridin-3-yl) thiazole-5-carbohydrazide, *International Journal of Corrosion and Scale Inhibition*, **8**, 1035 (2019). Doi: http://dx.doi.org/10.17675/2305-6894-2019-8-4-14
20. H. J. Habeeb, H. M. Luaibi, T. A. Abdullah, R. M. Dakhil, A. A. Kadhum, A. A. Al-Amiery Case study on thermal impact of novel corrosion inhibitor on mild steel, *Case Studies in Thermal Engineering*, **12**, 64 (2018). Doi: https://doi.org/10.1016/j.csite.2018.03.005
21. T. A. Salman, Q. A. Jawad, M. A. Hussain, A. A. Al-Amiery, L. Mohamed, A. A. Kadhum, and M. S. Takriff, Novel ecofriendly corrosion inhibition of mild steel in strong acid environment: Adsorption studies and thermal effects, *International Journal of Corrosion and Scale Inhibition*, **8**, 1123 (2019). Doi: http://dx.doi.org/10.17675/2305-6894-2019-8-4-19
22. T. Koopmans, Ordering of wave functions and eigenenergies to the individual electrons of an atom, *Physica*, **1**, 104 (1933). Doi: https://doi.org/10.1016/S0031-8914(34)90011-2
23. Alamiery AA. Effect of Temperature on the Corrosion Inhibition of 4-ethyl-1-(4-oxo-4-phenylbutanoyl) thiosemicarbazide on Mild Steel in HCL Solution, *Letters in Applied NanoBioScience*, **11**, 3502 (2022). Doi: https://doi.org/10.33263/LIANBS112.35023508
24. A. Alamiery, Corrosion inhibition effect of 2-N-phenylamino-5-(3-phenyl-3-oxo-1-propyl)-1, 3, 4-oxadiazole on mild steel in 1 M hydrochloric acid medium: Insight from gravimetric and DFT investigations, *Materials Science for Energy Technologies*, **4**, 398 (2021). Doi: https://doi.org/10.1016/j.mset.2021.09.002
25. A. A. Alamiery, W. N. Wan Isahak, and M. S. Takriff, Inhibition of Mild Steel Corrosion by 4-benzyl-1-(4-oxo-4-phenylbutanoyl) thiosemicarbazide: Gravimetrical, Adsorption and Theoretical Studies, *Lubricants*, **9**, 93 (2021). Doi: https://doi.org/10.3390/lubricants9090093
26. Jamil DM, Al-Okbi AK, Hanon MM, Rida KS, Alkaim AF, Al-Amiery AA, Kadhim A, Kadhum AA. Carbethoxythiazole corrosion inhibitor: As an experimentally model and DFT theory, *Journal of Engineering and Applied Sciences*, **13**, 3952 (2018). Doi: http://dx.doi.org/10.36478/jeasci.2018.3952.3959
27. A. Y. Musa, W. Ahmoda, A. A. Al-Amiery, A. A. Kadhum, A. B. Mohamad, Quantum chemical calculation for the inhibitory effect of compounds, *Journal of Structural Chemistry*, **54**, 301 (2013). Doi: https://doi.org/10.1134/S0022476613020042
28. S. Al-Baghdadi, T. S. Gaaz, A. Al-Adili, A. A. Al-Amiery, M. S. Takriff, Experimental studies on corrosion inhibition performance of acetylthiophene thiosemicarbazone for mild steel in HCl complemented with DFT investigation, *International Journal of Low-Carbon Technologies*, **16**, 181 (2021). Doi: https://doi.org/10.1093/ijlct/ctaa050
29. A. Al-Amiery, T. A. Salman, K. F. Alazawi, L. M. Shaker, A. A. Kadhum, M. S. Takriff, Quantum chemical elucidation on corrosion inhibition efficiency of Schiff base: DFT investigations supported by weight loss and SEM techniques, *International Journal of Low-Carbon Technologies*, **15**, 202 (2020). Doi: https://doi.org/10.1093/ijlct/ctz074
30. T. A. Salman, K. F. Al-Azawi, I. M. Mohammed, S. B. Al-Baghdadi, A. A. Al-Amiery, T. S. Gaaz, A. A.Kadhum, Experimental studies on inhibition of mild steel corrosion by novel synthesized inhibitor complemented with quantum chemical calculations, *Results in Physics*, **10**, 291 (2018). Doi: https://doi.org/10.1016/j.rinp.2018.06.019

31. Y. Meng, W. Ning, B. Xu, W. Yang, K. Zhang, Y. Chen, L. Li, , X. Liu, J. Zheng, and Y. Zhang, Inhibition of mild steel corrosion in hydrochloric acid using two novel pyridine Schiff base derivatives: a comparative study of experimental and theoretical results, *RSC Advances*, *7*, 43014 (2017). Doi: https://doi.org/10.1039/C7RA08170G
32. N. K. Gupta, M. A. Quraishi, C. Verma, and A. K. Mukherjee, Green Schiff's bases as corrosion inhibitors for mild steel in 1 M HCl solution: experimental and theoretical approach, *Rsc Advances*, **6**, 102076 (2016). Doi: https://doi.org/10.1039/C6RA22116E
33. D. S. Zinad, M. Hanoon, R. D. Salim, S. I. Ibrahim, A. A. Al-Amiery, M. S. Takriff, A. A. Kadhum, A new synthesized coumarin-derived Schiff base as a corrosion inhibitor of mild steel surface in HCl medium: gravimetric and DFT studies, *International Journal of Corrosion and Scale Inhibiton*, **9**, 228 (2020). Doi: http://dx.doi.org/10.17675/2305-6894-2020-9-1-14
34. A. Hidroklorik, Schiff bases derived from isatin as mild steel corrosion inhibitors in 1 M HCl, *Malaysian Journal of Analytical Sciences*, **18**, 507 (2014). http://mjas.analis.com.my/wp-content/uploads/2018/10/18_3_3.html
35. A. G. Bedir, M. Abd El-raouf, S. Abdel-Mawgoud, N. A. Negm, and N. M. El Basiony, Corrosion Inhibition of Carbon Steel in Hydrochloric Acid Solution Using Ethoxylated Nonionic Surfactants Based on Schiff Base: Electrochemical and Computational Investigations, *ACS Omega*, **6**, 4300 (2021). Doi: https://doi.org/10.1021/acsomega.0c05476
36. B. Chugh, A. K. Singh, S. Thakur, B. Pani, H. Lgaz, I. M. Chung, R. Jha, and E. E. Ebenso, Comparative investigation of corrosion-mitigating behavior of thiadiazole-derived bis-schiff bases for mild steel in acid medium: experimental, theoretical, and surface study, *ACS Omega*, **5**, 13503 (2020). Doi: https://doi.org/10.1021/acsomega.9b04274
37. P. Kumari and M. Lavanya, Optimization of Inhibition Efficiency of a Schiff Base on Mild Steel in Acid Medium: Electrochemical and RSM Approach, *Journal of Bio-and Tribo-Corrosion*, **7**, 110 (2021). Doi: https://doi.org/10.1007/s40735-021-00542-3
38. H. J. Habeeb, H. M. Luaibi, T. A. Abdullah, R. M. Dakhil, A. A. H. Kadhum, and A. A. Al-Amiery, Case study on thermal impact of novel corrosion inhibitor on mild steel, *Case Studies in Thermal Engineering*, **12**, 64 (2018). Doi: https://doi.org/10.1016/j.csite.2018.03.005
39. D. S. Zinad, Q. A. Jawad, M. A. Hussain, A. Mahal, L. Mohamed, A. A. Al-Amiery, Adsorption, temperature and corrosion inhibition studies of a coumarin derivatives corrosion inhibitor for mild steel in acidic medium: gravimetric and theoretical investigations, *International Journal of Corrosion and Scale Inhibition,* **9**, 134 (2020). Doi: http://dx.doi.org/10.17675/2305-6894-2020-9-1-8
40. J. A. Yamin, E. A. Sheet, A. Al-Amiery, Statistical analysis and optimization of the corrosion inhibition efficiency of a locally made corrosion inhibitor under different operating variables using RSM, *International Journal of Corrosion and Scale Inhibition*, **9**, 502 (2020). Doi: http://dx.doi.org/10.17675/2305-6894-2020-9-2-6
41. T. A. Salman, D. S. Zinad, S. H. Jaber, M. Al-Ghezi, A. Mahal, M. S. Takriff, A. A. Al-Amiery, Effect of 1, 3, 4-thiadiazole scaffold on the corrosion inhibition of mild steel in acidic medium: an experimental and computational study, *Journal of Bio-and Tribo-Corrosion*, **5**, 48 (2019). Doi: https://doi.org/10.1007/s40735-019-0243-7
42. S. B. Al-Baghdadi, A. A. Al-Amiery, A. A. Kadhum, and M. S. Takriff, Computational Calculations, Gravimetrical, and Surface Morphological Investigations of Corrosion Inhibition Effect of Triazole Derivative on Mild Steel in HCl, *Journal of Computational and Theoretical Nanoscience*, **17**, 2897 (2020). Doi: https://doi.org/10.1166/jctn.2020.9328
43. M. M. Hanoon, Z. A. Gbashi, A. A. Al-Amiery, A. Kadhim, A. A. Kadhum, M. S. Takriff, Study of Corrosion Behavior of N'-acetyl-4-pyrrol-1-ylbenzohydrazide for Low-Carbon Steel in the Acid Environment: Experimental, Adsorption Mechanism, Surface Investigation, and DFT Studies, *Progress in Color, Colorants and Coatings*, **15**, 133 (2022). Doi: https://dx.doi.org/10.30509/pccc.2021.166836.1118
44. M. M. Hanoon, A. M. Resen, A. A. Al-Amiery, A. A. Kadhum, M. S. Takriff, Theoretical and Experimental Studies on the Corrosion Inhibition Potentials of 2-((6-Methyl-2-Ketoquinolin-3-yl) Methylene) Hydrazinecarbothioamide for Mild Steel in 1 M HCl, *Progress in Color, Colorants and Coatings*, **15**, 11 (2022). Doi: https://dx.doi.org/10.30509/pccc.2020.166739.1095